

Biomed. Technik  
44 (1999), 272-277

M. Hentschel<sup>1</sup>  
J. Oellinger<sup>1</sup>  
C. Siewert<sup>1</sup>  
H. Wieder<sup>1</sup>  
N. Hosten<sup>1</sup>  
O. Wendt<sup>3</sup>  
T. Lüth<sup>2</sup>  
U. Boenick<sup>3</sup>  
R. Felix<sup>1</sup>

## <sup>1</sup>H and <sup>31</sup>P NMR Characterisation of a Double Breast Coil for Spectroscopic Measurements and Imaging

Charakteristik einer neu entwickelten Mammadoppelspule für die NMR Spektroskopie (<sup>1</sup>H/<sup>31</sup>P) und Bildgebung

University Hospital Charité, Campus Virchow Clinic, Humboldt University at Berlin

<sup>1</sup>Department of Radiology, Managing Director Prof. Dr. Dr. h. c. R. Felix

<sup>2</sup>Department of Head and Neck Surgery, Managing Director Prof. Dr. T. Lüth

<sup>3</sup>Technical University Berlin, Department of Biomedical Engineering, Managing Director Prof. Dr. U. Boenick

**Key words:** MR spectroscopy (MRS) – double breast coil – MR imaging (MRI)

For the first time a double turn breast coil has been described which can be used for <sup>1</sup>H imaging, <sup>1</sup>H spectroscopy and <sup>31</sup>P spectroscopy. The paper describes basic technical features of the coil, coil design, B<sub>1</sub> field/excitation field distribution for <sup>1</sup>H and <sup>31</sup>P, sensitivity, and feasibility for <sup>31</sup>P spectroscopic in vivo studies. The main advantage of the double frequency tuneable coil is that <sup>1</sup>H imaging for tumor localization and <sup>31</sup>P spectroscopy for response control can be done without an additional repositioning of the patient.

**Schlüsselwörter:** MR-Spektroskopie (MRS), Mammadoppelspule, MR-Bildgebung (MRI)

Erstmalig wird eine Mammadoppelspule beschrieben, die für die <sup>1</sup>H-Bildgebung sowie für die <sup>1</sup>H- und <sup>31</sup>P-Spektroskopie verwendbar ist. Diese Arbeit beschreibt die grundlegenden technischen Merkmale der Spule, das Spulendesign, das B<sub>1</sub>-Feld mit Anregung, die Feldverteilung für <sup>1</sup>H- und <sup>31</sup>P, die Sensitivität und die Durchführbarkeit der <sup>31</sup>P-Spektroskopie in vivo. Der wesentliche Vorteil der für zwei Frequenzen abstimmbaren Mammadoppelspule liegt in der <sup>1</sup>H-Bildgebung zur Tumorkalisation und der Möglichkeit der <sup>31</sup>P-Spektroskopie zur Kontrolle der Tumorsprechrate bei Patientinnen unter Chemotherapie. Diese Untersuchungen können ohne Umlagerung der Patientin durchgeführt werden.

### 1 Introduction

In recent years magnetic resonance spectroscopy (MRS) has gained in importance in medicine as a technique for investigating tissue and organ metabolism. Spectroscopy is a non-invasive technique which permits conclusions about physiological and pathological metabolic processes in tissues and organs in vivo. In contrast to magnetic resonance imaging (MRI), MRS is not yet an established clinical procedure. Various studies have been published in which MRS has been used to determine the metabolic status of certain tissues and for therapy monitoring, e.g. in chemotherapy, radiation treatment and hyperthermia [1, 2, 3, 4, 5].

Magnetic coils produce the alternating, high frequency (HF) magnetic field necessary for nuclear resonance excitation and detection of the HF field irradiated by the sample. They are the components of any MR system involved in direct exchange with the object being investigated [6].

To our best knowledge no double breast coil for

both <sup>1</sup>H imaging and <sup>31</sup>P spectroscopy is available commercially or has even been described in the literature until now. The coils currently used for spectroscopy are mostly surface coils [7, 8].

The present work describes for the first time a double turn breast coil which can be used for <sup>1</sup>H imaging, <sup>1</sup>H spectroscopy and <sup>31</sup>P spectroscopy. The paper describes basic technical features of the coil, coil design, B<sub>1</sub> field/excitation field distribution for <sup>1</sup>H and <sup>31</sup>P, sensitivity, and feasibility for <sup>31</sup>P spectroscopic in vivo studies. The main advantage of the double frequency tuneable coil is that <sup>1</sup>H imaging for tumor localization and <sup>31</sup>P spectroscopy for response control can be done without an additional repositioning of the patient.

### 2 Materials and Methods

All the MR investigations were conducted employing a commercial MR scanner (Magnetom 63/83 SP, 1.5T, Siemens AG, Erlangen) at the University Medical Cen-

Bereitgestellt von | Technische Universität Berlin

Angemeldet

Heruntergeladen am | 09.11.18 17:25

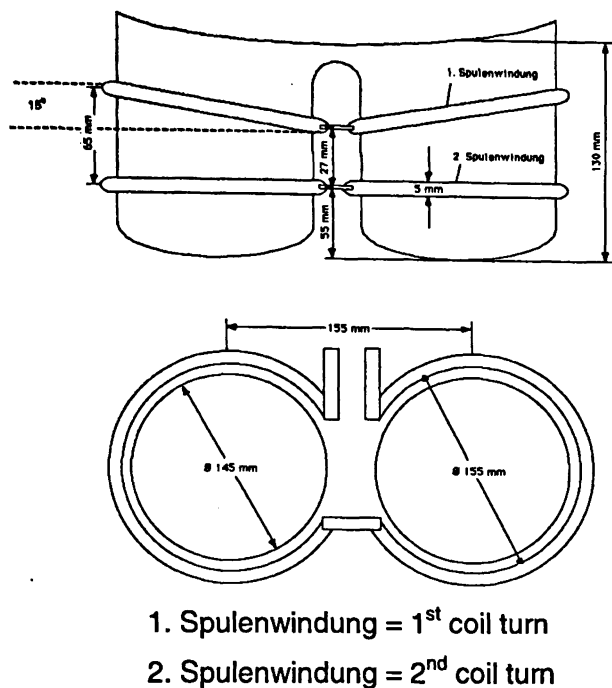


Fig. 1. Geometric design of the double breast coil with the arrangement of the coil turns. (1. Spulenwindung = 1<sup>st</sup> coil turn, 2. Spulenwindung = 2<sup>nd</sup> coil turn)

ter, Campus Virchow Clinic of the Medical Faculty of the Humboldt University in Berlin. The resonance frequencies were: 63.3 MHz for  $^1\text{H}$  and 25.7 MHz for  $^{31}\text{P}$ . A double turn breast coil from Siemens Company was redesigned so that, in addition to MR imaging,  $^{31}\text{P}$  MR spectroscopic investigations ( $^1\text{H}$  and  $^{31}\text{P}$  spectroscopy) could be carried out. In all investigations the breast coil was used for both transmission and detection.

## 2.1 Coil Design

The coil consists of two figure-eight turns ( $d = 155$  mm, Fig. 1) made of copper tubing (thickness: 5 mm), which are located one above the other and connected either in parallel ( $^1\text{H}$  frequency) or in series ( $^{31}\text{P}$  frequency). The two turns surround two cylindrical cups at a radial distance of 5 mm (height: 130 mm; inner diameter: 145 mm) which for placement of the patient's breasts during the investigation. The lower turn is at a distance of 55 mm from the bottom of the cup and is parallel to it. The upper turn is in the middle between the two cups at a distance of 27 mm from the lower turn, is slanted upwards at an angle of  $15^\circ$  and has an externally distance of 65 mm from the lower turn. The switching is achieved by high-ohmic, pretuned rejection circuits for the signal in the corresponding frequency range (63.3 MHz for  $^1\text{H}$  or 25.7 MHz for  $^{31}\text{P}$ ), allowing the measurements of  $^1\text{H}$  or  $^{31}\text{P}$  without the need for a switch. Parallel connection of the two turns corresponds to the high resonance frequency (Fig. 2a:  $^1\text{H}$ ) and series connection of the two turns corresponds to the low resonance frequency (Fig. 2b:  $^{31}\text{P}$ ). The reso-

nance matching (C2) and tuning (C1) capacitors have been selected so that for a loaded coil they permit a resonance matching to  $50\ \Omega$  and a tuning to 63.3 or 25.7 MHz. There was no additional symmetrification of the matching circuit. The quality factor ( $Q$ ) of the coil under loaded conditions (1L 0.1 mol  $\text{H}_3\text{PO}_4$ ) was approximately 115 for 63.3 MHz and 190 for 25.7 MHz.

## 2.2 $^1\text{H}$ Imaging

Firstly, the breast coil was used for  $^1\text{H}$  imaging to measure the  $B_1$  field distribution of the coil. Suitable phantoms consist simply of two 2L water bottles ( $d = 120$  mm;  $h = 245$  mm) which were placed directly into the two cups of the breast coil. For determining the transmitter voltage for a  $90^\circ$  pulse the phantoms were placed into the coil and the transmitter voltage was varied between 0 and 90 V. Standard gradient-echo sequences were used with  $T_R = 20$  ms,  $T_E = 11$  ms, slice thickness = 4 mm, acquisition number = 1, FOV = 350 mm, matrix size =  $192 \times 256$ , corresponding to a planar resolution of  $1.8\text{ mm} \times 1.4\text{ mm}$ . 2D images in coronal, sagittal and transverse orientation through the phantom were taken to obtain the  $B_1$  field distribution in the corresponding orientation. Image analysis was carried out on a Macintosh Power PC (8100/80) using the program package NIH Image 1.54 (Institute of Health, Bethesda, USA).

No  $^{31}\text{P}$  imaging was performed due to the low sensitivity of the  $^{31}\text{P}$  nucleus. However, to measure the  $B_1$  field distribution for this frequency as well  $^{31}\text{P}$  spectroscopy was used.

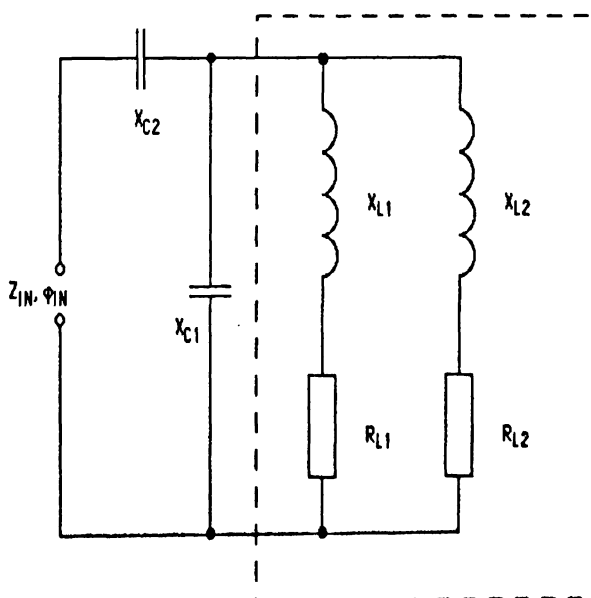


Fig. 2a. Circuit diagram of the parallel connection of the coil turn.

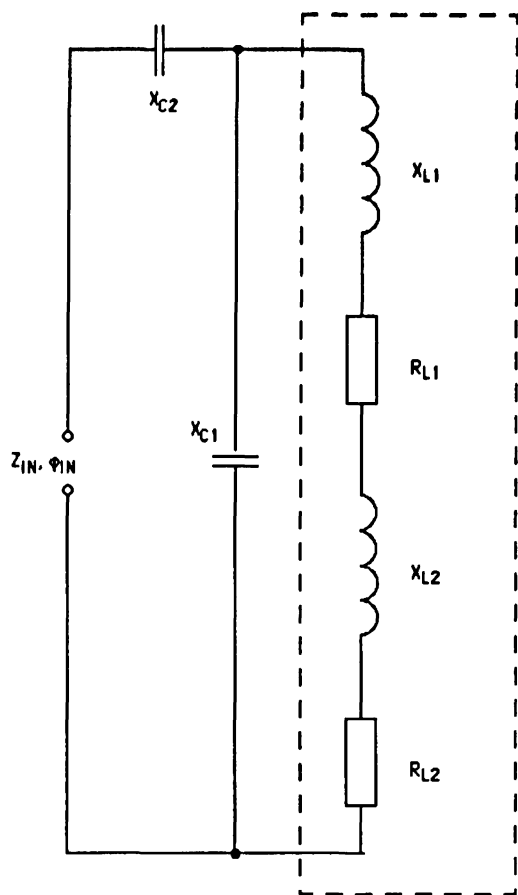


Fig. 2b. Circuit diagram of the series connection of the coil turn.

### 2.3 $^{31}\text{P}$ Spectroscopy

For this purpose special phantoms have to be developed. For the investigations in the coronal and sagittal planes six acrylic glass tubes (maximal area of the cross section:  $78\text{ cm}^2$ , minimal area:  $0.78\text{ cm}^2$ ) were attached concentrically to a baseplate, (Fig. 3a). For the actual  $^{31}\text{P}$  measurement a pipette closed at its lower end containing  $0.1\text{ mol H}_3\text{PO}_4$  (pure, Sigma, Ger-

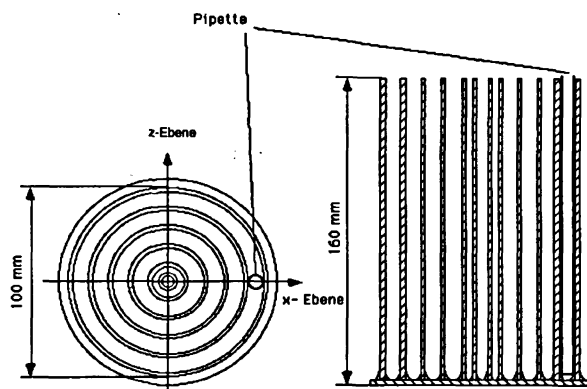


Fig. 3a.  $^{31}\text{P}$  phantom for investigation in coronal and sagittal planes.

many) with a total volume of  $10\text{ ml}$  was used. To ensure a constant loading the whole ring phantom was filled to the very top with water. The pipette was then moved into the coronal or sagittal plane depending on the orientation in question either from right to left or top to bottom (cranial to caudal). In each position of the pipette (four for each ring) the dependence of the signal intensity on the transmitter amplitude (the transmitter amplitude profile) was recorded.

For the measurements in the transverse plane Petri dishes were used which were placed on top of each other to give a constant height of  $120\text{ mm}$  (Fig. 3b). At the beginning the phosphoric acid was in the lowest Petri dish; this dish was then moved upwards one level after each transmission amplitude profile was recorded. All the  $^{31}\text{P}$  spectroscopic experiments were measured using a simple transmit receive sequence (FID). The other measuring parameters were:  $T_R = 1500\text{ ms}$ ,  $T_D = 500\text{ }\mu\text{s}$ ,  $D_{\text{well Time}} = 500\text{ ms}$ , Sample Width =  $1000\text{ Hz}$ , Vector Size =  $1024$ , Acquisitions =  $1$  to  $1024$  (variable), Transmitter Amplitude = variable, Receiver Gain =  $95\text{ dB}$ .

Evaluation of the spectroscopic results was done using the standard spectroscopy software package from Siemens, as well as software developed by us (adapted for Igor Pro, Wave Metrics, USA).

For determining the transmitter voltage for a  $90^\circ$  pulse for  $^{31}\text{P}$  a  $1\text{ L } 0.1\text{ mol H}_3\text{PO}_4$  phantom was placed in the right or left cup of the coil, with a water phantom being placed in the other cup, and then the transmitter voltage was varied over the range  $0$  to  $90\text{ V}$ . The investigation was repeated with a  $1\text{ L } 0.1\text{ mol}$  phosphoric acid phantom in both cups.

### 3 Results

Since the primary interest is in using the coil for in vivo measurements the shim and imaging were conducted first at a proton frequency of  $63.3\text{ MHz}$ . At the start of the shim procedure inhomogeneities of the main magnetic field ( $B_0$ ) usually led to two peaks in the

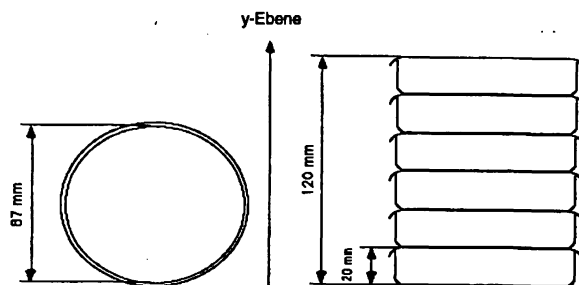


Fig. 3b.  $^{31}\text{P}$  phantom for investigation in a transverse plane

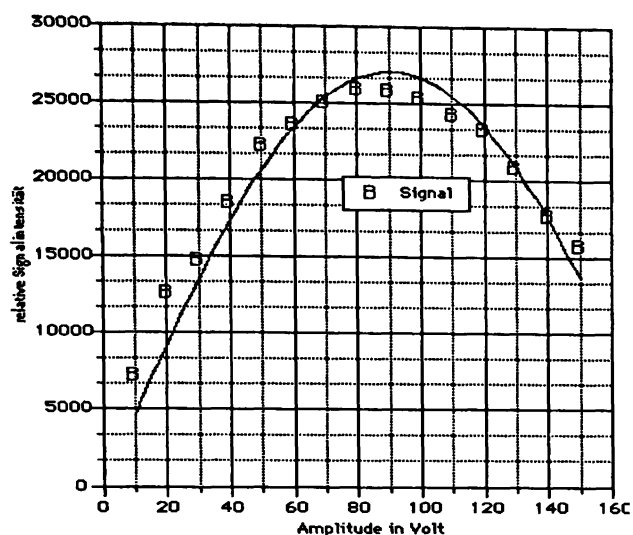


Fig. 4.  $^1\text{H}$  transmitter profile of a 1 liter water phantom.

spectrum of the water phantom, which have to be brought in coincidence by suitable choice of the shim currents. Typical water line width of  $\approx 10$  Hz were reached in about 5 minutes.

### 3.1 $^1\text{H}$ Imaging

Figure 4 shows the  $^1\text{H}$  excitation profile of a water phantom in dependence on the transmitter voltage and the corresponding measured relative signal intensity. The maximum is attained at a transmitter voltage of 85 V ( $\pm 5$ ).

For practical reasons, the following descriptions are based on a 3-dimensional coordinate system with the  $z$ -axis running through the midpoint of the figure-eight coil turns and the origin ( $x = y = z = 0$ ) at the base of the cup. The  $x, z$  coordinate plane is the coronal plane, the  $x, y$  coordinate plane is the transverse plane and the  $y, z$  coordinate plane is the sagittal plane.

For the  $x, z$  plane a coronal surface plot was placed

through the water phantom (Fig. 5). At the outer right and left edges of the coil ( $x$ -axis) the relative signal intensity was highest (defined as 100 %); it decreased continuously with increasing distance from the coil turns to a relative signal intensity of 30 % at the medial edge of the water phantom. Along the  $z$ -axis the maximum relative signal intensity of 100 % was at 0 cm; this decreased cranial and caudal to 10 % at  $-6$  cm and  $+6$  cm.

For the  $x, y$  plane (transverse plane) the same procedure was used. A transverse surface plot was placed through the water phantom (Fig. 6). The intensity distribution of the relative signal intensity along the  $y$ -axis shows a maximum of 100 % at 4 cm and 13 cm, which declines in the right water phantom to 80 % at  $-8$  cm and in the left water phantom to 70 % at 8 cm.

For the  $y, z$  plane a sagittal surface plot was placed through the water phantom (Fig. 7). As it is clear from Fig. 7a relative signal intensity along the  $y$ -axis of 100 % is reached at 4 cm and 12 cm, which decreases to 90 % at 8 cm. Along the ventral axis the signal intensity decreases to 77 %. Cranial the signal is no longer measurable at 5 cm.

### 3.2. $^{31}\text{P}$ Spectroscopy

Figure 8 shows the relative signal amplitude of the 0.1 M  $\text{H}_3\text{PO}_4$  phantom in dependence on the transmitter voltage. The maximum is obtained at a voltage of 65 V ( $\pm 5$ ). This is true both for the individual coil halves and for the two coil halves taken together.

#### 3.2.1 $B_1$ Field Distribution

The results with respect to the  $B_1$  field distribution in the coronal plane are given in Fig. 9a. In  $^{31}\text{P}$  spectroscopy a clear loss in signal can be observed in the coronal plane in the direction of the center of the coil. The relative signal intensity drops for both cups from 100 % in the lateral coil regions to about 50 % in the medial part of the coil. The following results were ob-

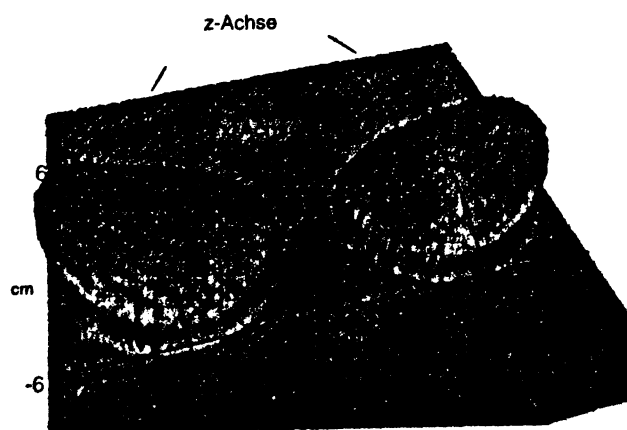


Fig. 5. Coronal surface plot through two water phantoms.

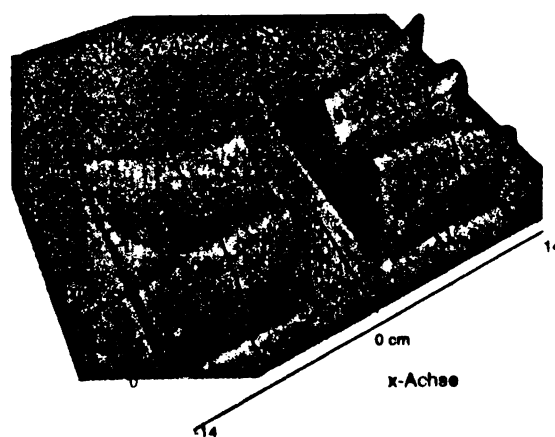


Fig. 6. Transverse surface plot through two water phantoms.

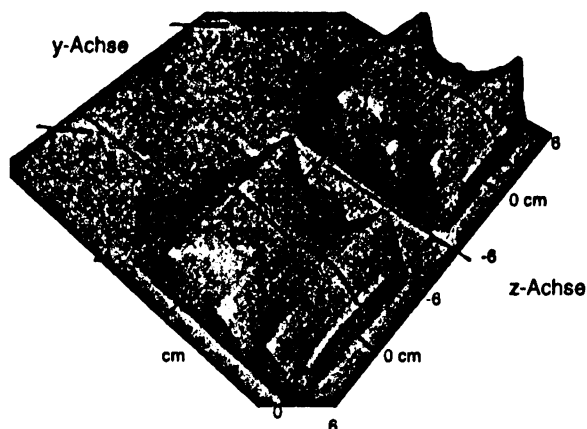


Fig. 7. Sagittal surface plot through two water phantoms.

tained in the transverse plane (Fig. 9b). There is a clear maximum signal intensity of 100 % at about 5 cm along the z-axis. Ventral and dorsal there is a clear reduction in signal intensity to about 60 % at 0 cm and 50 % at 12 cm, respectively. The relative signal intensity maximum of 100 % in the sagittal plane is in the middle, dropping cranial and caudal to 70 %.

### 3.2.2 Detection Limit

The spectroscopic detection limit of the breast coil (signal-to-noise ratio (SNR)  $\leq 3$ , measuring time  $\leq 30$  min, intratumoral concentration ( $\leq 5$  mM) was measured with a phantom we developed ourselves: a small vial (height about 40 mm; diameter = 1 cm) was repeatedly filled with decreasing concentrations of  $\text{H}_3\text{PO}_4$  and placed in a 2 L bottle filled with water. The detection limit was reached at about 5 mM.

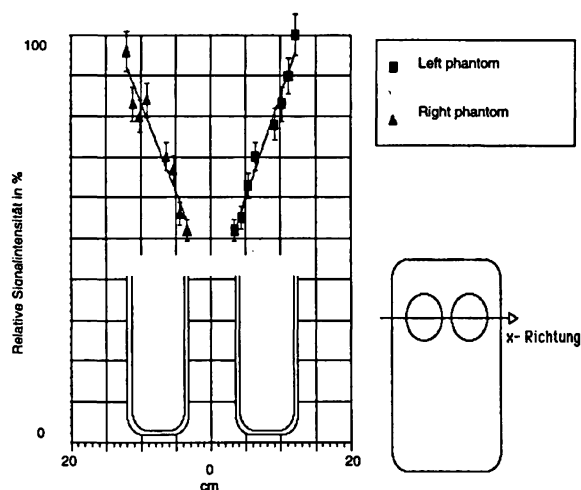
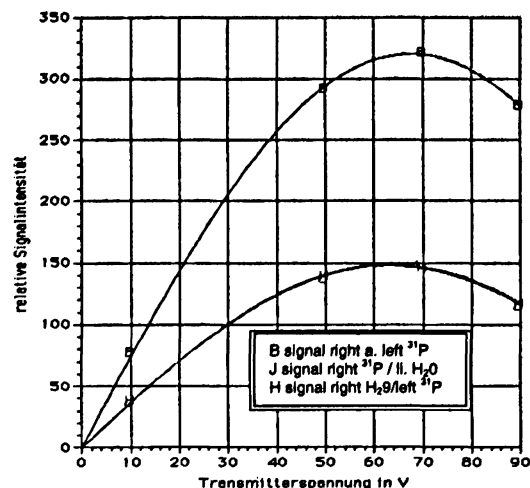


Fig. 9a. Relative signal intensity of a 1M phosphorous phantom in a coronal plane at a transmitter voltage of 70 V.

Fig. 8.  $^{31}\text{P}$  transmitter profile for a 0.1M phosphorous phantom.

### 4 In-vivo Results

In a clinical study 20 patients with primary inoperable breast carcinoma underwent a neo-adjuvant chemotherapy. In order to monitor the course of the treatment the patients were investigated before chemotherapy and two to five times during the course of the chemotherapy treatment with  $^1\text{H}$  MR tomography and  $^{31}\text{P}$  MR spectroscopy (MRI), with a total of 72  $^1\text{H}$  MRT and 72  $^{31}\text{P}$  MRS investigations being carried out [13]. The  $^{31}\text{P}$  MRS spectra comprised 7 resonances [ $\alpha$ -,  $\beta$ -, and  $\gamma$ -adenosine triphosphate (ATP), phosphocreatine (PCr), inorganic phosphate (Pi), phosphomonoester (PME) and phosphodiester (PDE) which have been shown to be present in malignant tumors in other in-vivo  $^{31}\text{P}$  MRS studies of the breast [9, 10, 11, 12]. Combining  $^1\text{H}$  MRI with  $^{31}\text{P}$  MRS it was possible to show a positive response to chemotherapy.

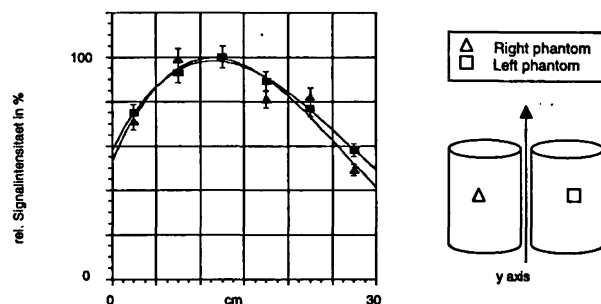


Fig. 9b. Relative signal intensity in a transverse plane at a transmitter voltage of 70 V.

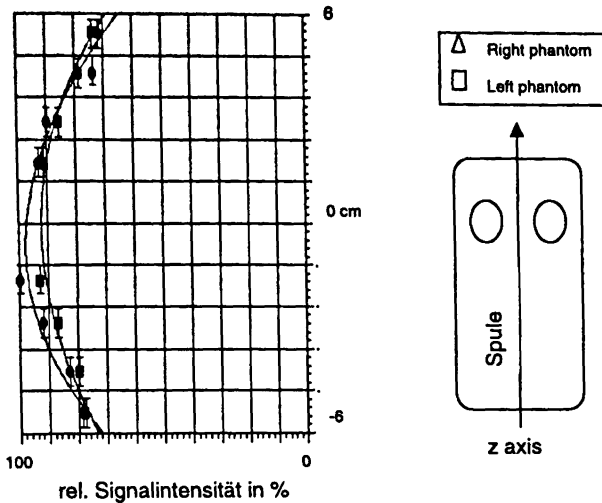


Fig. 9c. Relative signal intensity in a sagittal plane at a transmitter voltage of 70 V.

## 5 Discussion

The newly developed, two-fold tuneable double breast coil for  $^1\text{H}$  imaging and  $^{31}\text{P}$  spectroscopy was evaluated as to its MR properties; in particular,  $B_1$  field/excitation field distribution for  $^1\text{H}$  and  $^{31}\text{P}$ , sensitivity, and feasibility for  $^{31}\text{P}$  spectroscopic in vivo studies.

In  $^1\text{H}$  imaging the volume within which the coil can detect a signal with intensity of approx. 90 % of the maximum was  $50\text{ cm}^3$  for the right cup and  $52\text{ cm}^3$  for the left cup. For  $^{31}\text{P}$  spectroscopy the volume within which an isointense signal ( $\approx 90\%$ ) was observed was about two times smaller. It equals  $20\text{ cm}^3$  for the right cup and  $15\text{ cm}^3$  for the left cup. The difference is not well understood at the moment but maybe caused by the much lower sensitivity of the  $^{31}\text{P}$  nucleus.

Furthermore, there are two more reasons for non-uniformity of  $B_1$  field distribution in the double breast coil. At first, since the coil turns do not form a closed circle but rather a figure-eight turn there is a lower concentration of the magnetic field lines in the center of the coil, leading to a decrease in the signal there. Secondly, a depletion of the signal for both  $^1\text{H}$  MRI and  $^{31}\text{P}$  MRS was observed in the immediate vicinity of the coil turns. In these areas the HF pulse reaches values near  $180^\circ$  so that those spins do not contribute to the observable net magnetization ( $M_{xy}$ ).

The  $B_1$  field distribution obtained by the  $^{31}\text{P}$  spectroscopic investigations showed a complex pattern. The signal intensity decrease along the  $x$ -axis in the direction of the coil center and shows a maximum signal intensity along the  $y$ -axis at the level of the lower coil turn. Along the  $z$ -axis the maximum was observed in the center, which dropped off uniformly to both sides.

If the present coil is used to measure a non-localized  $^{31}\text{P}$  MR spectrum by averaging over the volume of

both mammae, the spectrum measured will be a superposition of different tissue species. It will contain portions from the tumor, healthy breast and muscle tissue (M. pectoralis). These different tissue types have (very) different concentrations of phosphorous metabolites. In addition, the different  $B_1$  field and signal strength in different parts of the volume of interest have also be taken into account. Despite these considerations it seems possible to detect the response of tumors to chemotherapy at an early stage, when the size of the tumor has not yet been changed considerably[13]. As the latter can be confirmed easily by parallel  $^1\text{H}$  imaging the double tuneable breast coil maybe considered as useful for treatment evaluation in the described measurement scenario.

## References:

- [1] Glaholm, J.; M. O. Leach et al.: In-vivo  $^{31}\text{P}$  magnetic resonance spectroscopy for monitoring treatment response in breast cancer. *The Lancet* (1989), 1326-1327.
- [2] Renmond, O. M.; J. P. Stack et al.: In vivo phosphorus-31 magnetic resonance spectroscopy of normal and pathological breast tissues. *The british Journal of Radiology* 64 (1994), 10-216.
- [3] Sijens, P. E.; H. K. Wijrdeman et al.: Human breast cancer in vivo: H-1 and P-31 MR-Spectroscopy at 1.5 T. *Radiology* 169 (1988), 615-620.
- [4] Kalra, R.; K. E. Wade et al.: Phosphomonoester is associated with proliferation in human breast cancer: A  $^{31}\text{P}$  MRS study. *Br. J. Cancer* 67 (1993), 1145-1153.
- [5] Redmond, O. M.; J. P. Stack et al.:  $^{31}\text{P}$  MRS as an early prognostic indicator of patient response to chemotherapy Magnetic resonance in *Medicine* 25 (1992), 30-44.
- [6] Hentschel, M.; M. Wust et al.: Spektroskopische Eigenschaften einer interstitiellen Miniaturantenne für die  $^{31}\text{P}$ -MRS. *Strahlenther. Oncol.* 172 (1996), 610-618.
- [7] Knopp, M. V.; T. Heß et al.: Magnetresonanztomographie des Mammakarzinoms. *Radiologe* 33 (1993), 300-307.
- [8] Lowry, M.; D. A. Porter et al.: Visibility of phospholipids in  $^{31}\text{P}$  NMR spectra of human breast tumours in vivo. *NMR in Biomedicine* 5 (1992), 37-42.
- [9] Merchant, T. E.; L. W. Gierke et al.:  $^{31}\text{P}$  Magnetic resonance spectroscopy profiles of neoplastic human breast tissues. *Cancer Research* 48 (1988), 5112-5118.
- [10] Twelves, C. J.; M. Lowry et al.: Phosphorus-31 metabolism of human breast - an in vivo magnetic resonance spectroscopic study at 1.5 tesla. *The British Journal of Radiology* 67 (1994), 36-45.
- [11] Twelves, C. T.; D. A. Porter et al.: Phosphorus-31 metabolism of post-menopausal breast cancer studied in vivo by magnetic resonance spectroscopy. *Br. J. Cancer* 69 (1994), 1151-1156.
- [12] Thian, C. N. G.; S Grundfest et al.: Therapeutic response of breast carcinoma monitored by  $^{31}\text{P}$  MRS in situ. *Magnetic Resonance in Medicine* 10 (1989), 125-134.
- [13] Oellinger, J.; Blohmer et al.: Combined  $^1\text{H}$  MRI and  $^{31}\text{P}$  MRS study for treatment evaluation during chemotherapy: First clinical results. (Submitted to *Breast*).

919

Korrespondenzanschrift:  
Dr. med. J. Oellinger/MRT-Labor  
Universitätsklinikum Charité  
Strahlenklinik und Poliklinik  
Campus Virchow Klinikum  
Humboldt Universität zu Berlin  
Augustenburger Platz 1  
D-13353 Berlin